Assessment of neutron emission from DD to DT operation of ITER

A.R. Polevoi[1], A. Loarte[1], R. Bilato[2], L. Bertalot[1], R.V. Budny[3], E. Fable[2], M. Gorelenkova[3], M. Loughlin[1], E. Polunovskiy[1]

[1]*ITER Organization, Route de Vinon-sur-Verdon, 13067 St Paul Lez Durance, France*

[2]*Max-Planck-Inst. für Plasmaphysik, Boltzmannstr.2, 85748 Garching, Germany,*

[3]*PPPL, Princeton University, Princeton, NJ 08543-0451, USA*

1. Introduction

An assessment of the 2.45 and 14 MeV neutron yield and neutron emission spatial distributions for the DD and DT phases of ITER operation is needed to define the details of a set of dedicated experiments to be carried out in order to establish the reliability of the neutronics calculations early in ITER nuclear operations [1] and to evaluate the capabilities and performance of the ITER neutron diagnostics in different phases/scenarios during ITER nuclear operation. The main challenge for these two issues is that the evaluations of the capability/reliability are foreseen to be carried out during the ITER DD operational phase (or early in the DT phase) when the neutron flux and fluence will be orders of magnitude lower than those expected at Q = 10.

2. Transport model

In our analysis we use self-consistent 1.5D simulations in the frame of ASTRA [2] with the scaling based transport model [3]. The boundary conditions are defined from SOLPS predictions for ITER operation with the tungsten divertor, and the pedestal parameters for H-mode plasmas are evaluated with the EPED1 model and the SOLPS-based boundary conditions [4]. For each set of operational conditions the electron and ion heat conductivities were fitted to the appropriate scaling: Ohmic [5], L-mode and H-mode [6]. For particle diffusivity we used the same assumption for all species, $D = D_e = 0.2\ \chi_{eff} = 0.1\ (\chi_e + \chi_i)$, based on JET experiments for the ITER-like conditions [7]. As noted in the ref. [7], this choice of D is lower than the tritium diffusivity obtained in the JET tritium trace experiments, ($D_T \sim 0.3 - 2\ \chi_{eff}$) or in the analysis of H-mode density profiles from multimachine databases [8] ($D_T \sim 0.4 - 0.7\ \chi_{eff}$). Thus, our estimate of tritium accumulation in DD plasma is conservative. In the simulations, together with the reactions between the thermal D and T ions, we take into account interaction of the fast D ions from the 1 MeV ITER NBI and the 1 MeV tritium produced from the DD reaction with the thermal D and T ions in approximation of finite electron and ion temperatures. The probability of the fusion reaction of a fast

ion with energy E_A with a thermal specie "B" during slowing down is given by $F_{AB}(E_A,T_i,T_e)= n_e \int<\sigma_{AB}V> dt = n_e \int<\sigma_{AB}V> E^{-1} \tau(E,T_i,T_e)\, dE$, where $\tau(E,T_i,T_e) \sim 1/n_e$ is the slowing down time, $dE/dt = -E/\tau(E,T_i,T_e)$, and <…> denotes averaging over the thermal species Maxwellian distributions. The source of the 14 MeV neutrons, S_{n14}, from DT reaction, D+T → n + ^{4}He, is given by $S_{n14} = n_{Tth}n_{Dth}\, S_{DT} + S_T\, F_{TD}\, n_{Dth}/n_e + S_{DNB}\, F_{DT}\, n_{Tth}/n_e$, where $S_{DNB}[10^{19}/s]=P_{NB}[MW]/1.6$ with P_{NB} is the 1 MeV NBI absorbed power, n_{Tth} , n_{Dth}, n_e are the densities of the thermal T and D ions and electrons and S_T is the source of 1.008 MeV T from the DD reaction both from reaction of thermal D-D and from D-fast D from NBI DD1: D+D (50%) → T + p ($S_T = 0.5\, n_{Dth}^2\, S_{DD1} + S_{DNB}\, F_{DD1}\, n_{Dth}/n_e$). The source of 2.45 MeV neutrons, $S_{n2.45}$, from the DD (thermal DD + thermal-fast NBI D) reaction DD2: D+D (50%) → $n_{2.45}$ + ^{3}He, is given by $S_{n2.45} = 0.5\, n_{Dth}^2\, S_{DD2} + S_{DNB}\, F_{DD2}\, n_{Dth}/n_e$. The temperature dependence of the fusion rates and the probabilities of burn during fast particles slowing down are shown in Fig. 1 (a, b) with the expected increase of the ratio of thermal to slowing-down fusion rates S_{DT}/F_{DT} with temperature (Fig.1 (a)). The fusion probabilities for fast particles take into account the finite value of the ion temperature both for DD and DT. To evaluate them we have extended the technique, proposed in [9] for DD, to DT plasmas keeping all terms of order $\varepsilon = T_i/E_A << 1$ omitted in [9]. This improved formulation leads to different fusion probabilities for fast particles at high T_i in comparison with those evaluated for cold ions (see Fig. 1 (c)), as expected.

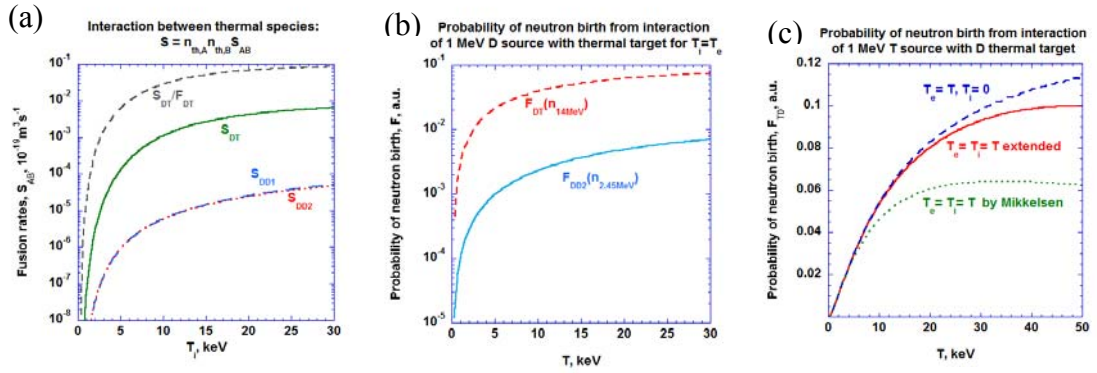

Figure 1. Fusion rates for thermal species (a), probabilities of the fast ion reactions with thermal species during the slowing down (b), probability of fast ion reactions during slowing down of 1.008 MeV T on thermal D ions.

3. Code benchmarking

The simulations with ASTRA [2] and a simplified NBI description [10] have been successfully benchmarked with simulations from TRANSP+NUBEAM [11], which uses a Monte-Carlo technique for description of fast ions, as shown in Fig. 2. (a, b) for

a 12 MA ITER plasma with 33 MW of NBI power and $n_D = n_T$. In these conditions the 14 MeV neutron source from the fast D(NBI)-thermal T reaction is negligible compared to the thermal DT source while the 2.45 MeV neutron source from fast D(NBI)-thermal D reactions is comparable to that of the thermal DD reaction in these conditions (Fig. 2 (c)).

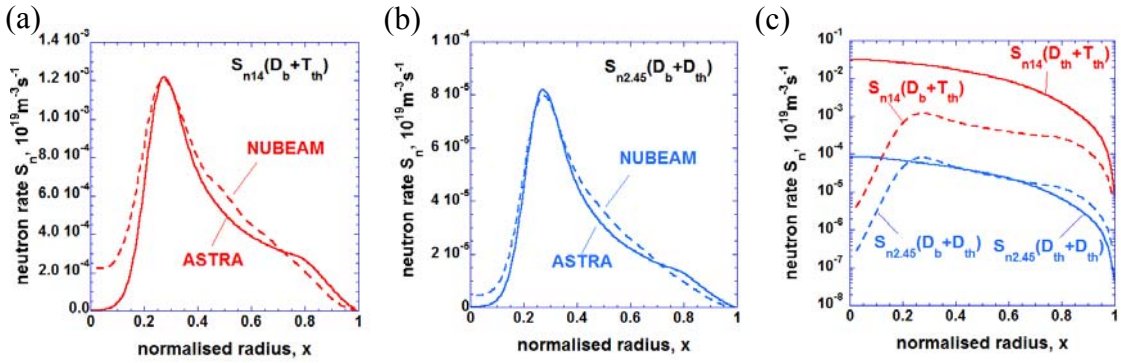

Figure 2. Comparison of the neutron sources predicted by ASTRA and TRANSP+NUBEAM for ITER plasma with 33 MW of 1 MeV D-NBI and $n_D=n_T$. N neutron sources from the DT reaction and DD reactions: S_{n14}(Fig. 2 (a)) and $S_{n2.45}$(Fig. 2 (b)). Neutron sources predicted by TRANSP+NUBEAM for the thermal-thermal and fast-thermal fusion reactions (Fig.2 (c)).

4. ITER simulations

Our assessment includes ITER DD and DT plasmas in Ohmic, L-mode and H-mode with full (5.3T) and half (2.65T) toroidal field and plasma currents 7.5 – 17 MA.

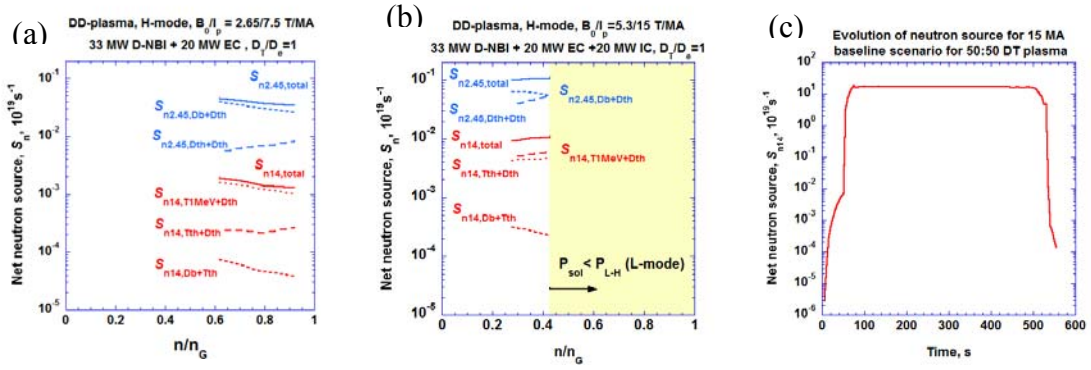

Figure 3. Neutron production versus normalized plasma density for DD H-mode plasmas with I_p = 7.5 MA (Fig. 3(a)), I_p= 15 MA (Fig.3.(b)) and 14 MeV neutron production rate versus time for the 15 MA Q=10 DT scenario (Fig. 3(c)).

The DD plasma results for $S_n = \int S_n dV$ shown in Fig. 3 (a, b) assume zero T recycling because of the low amount of T produced. Increasing T recycling in these conditions up to 100% leads to a doubling of the edge T density and to an increase of the total T content by 30% in H-mode. This leads to an increase by 30% of the thermal T sources for 14 MW neutrons compared to the values in Fig.3. (a b). Increasing the T thermal diffusivity by a factor $K = D_t/D = 1.5 – 10$, as observed in the JET T-trace experiments [7], decreases the thermal T content and thermal 14 MeV neutron sources

as 1/K compared to the values in Fig.3. (a b). As shown in Fig. 3.a, for 7.5MA/2.65T DD plasmas the dominant 14 MeV neutron source is caused by the burn of 1 MeV T produced in the DD reaction (Fig. 1(a)) so that assumptions on T transport and recycling have little effect on the 14 MeV neutron rate in these conditions. The same applies to the 2.45 MeV neutron source which is dominated by the 1 MeV NBI-D reaction with the thermal D. For 15MA/5.3T DD plasmas, which have higher temperatures, the contribution from the thermal reactions the 14 MeV and 2.45 MeV neutrons increase and are comparable to those from fast particle-thermal reactions (Fig. 3 (b)) as expected from Fig. 1 (a) (see S_{DT}/F_{DT}). The typical neutron yields in DD and DT ITER Ohmic and H-mode plasmas are summarized in Table 1.

Table 1. Neutron yield at plasma current flat-top

B/I_p,T/MA	n_e,$10^{19}m^{-3}$	S_n,$10^{19}s^{-1}$	S_{n14}/S_n,%	n_T/n_e,%	P_{heat}/P_α,MW	mode
2.65/7.5	3	$1.06\ 10^{-5}$	0.8	$2.74\ 10^{-6}$	$7.5/4.64\ 10^{-7}$	OH/DD
2.65/7.5	3.6	0.0468	4	0.006	53/0.011	H/DD
5.3/15	3.3	0.1093	8.5	0.019	73/0.053	H/DD
5.3/15	11.2	17.45	~100	39.8	50/98	H/DT
5.3/17	12.5	25	~100	38.5	50/140	H/DT

Disclaimer. ITER is the Nuclear Facility INB no. 174. This paper simulates plasma physics processes, neutron production and fusion performance during ITER operation; nevertheless the nuclear operator is not constrained by the results of this paper. The views and opinions expressed herein do not necessarily reflect those of the ITER Organization.

References

[1] M. Loughlin, et al, Fusion Engineering and Design **89** (2014) 1865–1869
[2] G.V. Pereverzev, P.N. Yushmanov, "ASTRA Automated System for TRansport Analysis", IPP-Report IPP 5/98 (2002)
[3] A.R. Polevoi, et al, Plasma Phys. and Contr. Fusion **48** (2006) A449
[4] A.R. Polevoi, et al, Nucl. Fusion **55** (2015) 063019
[5] G. Bracco and K. Thomsen, Nucl. Fusion **37** (1997) 759
[6] ITER Physics Basis, 39 (1999) 2208
[7] M. Valovic, et al, Nucl. Fusion **47** (2007) 196-200
[8] C. Angioni, et al , Nucl. Fusion **47** (2007) 1326
[9] D.R. Mikkelsen, Nucl. Fusion **29** (1989) p. 1113
[10] A.Polevoi, H.Shirai, T.Takizuka,"Benchmark of the NBI Block in ASTRA Code versus the OFMC Calculations", JAERI-DATA-Code 97-014, JAERI, March 1997
[11] A. Pankin, et al., Computer Phys. Communications, Vol. 159, No. 3 (2004) 157-184